Organic & Biomolecular Chemistry

Dynamic Article Links

Cite this: *Org. Biomol. Chem.*, 2012, **10**, 1440

www.rsc.org/obc

PAPER

Solid state NMR studies of oligourea foldamers: Interaction of ^{15}N-labelled amphiphilic helices with oriented lipid membranes†

Christopher Aisenbrey,[a] Nagendar Pendem,[b] Gilles Guichard*[b] and Burkhard Bechinger*[a]

Received 28th July 2011, Accepted 25th October 2011
DOI: 10.1039/c1ob06278f

Synthetic oligomers that are derived from natural polypeptide sequences, albeit with unnatural building blocks, have attracted considerable interest in mimicking bioactive peptides and proteins. Many of those compounds adopt stable folds in aqueous environments that resemble protein structural elements. Here we have chemically prepared aliphatic oligoureas and labeled them at selected positions with ^{15}N for structural investigations using solid-state NMR spectroscopy. In the first step, the main tensor elements and the molecular alignment of the ^{15}N chemical shift tensor were analyzed. This was possible by using a two-dimensional heteronuclear chemical shift/dipolar coupling correlation experiment on a model compound that represents the chemical, and thereby also the chemical shift characteristics, of the urea bond. In the next step ^{15}N labeled versions of an amphipathic oligourea, that exert potent antimicrobial activities and that adopt stable helical structures in aqueous environments, were prepared. These compounds were reconstituted into oriented phospholipid bilayers and the ^{15}N chemical shift and ^{1}H-^{15}N dipolar couplings of two labeled sites were determined by solid-state NMR spectroscopy. The data are indicative of an alignment of this helix parallel to the membrane surface in excellent agreement with the amphipathic character of the foldamer and consistent with previous models explaining the antimicrobial activities of α-peptides.

Introduction

α-Peptides exert many important biological activities and have therefore been subject to a wide variety of biophysical and structural investigations. In particular, they are known to act as neurotransmitters, have antimicrobial and cell penetrating activities, or act as nucleic acid transfection agents.[1–5] Many of these, in particular the hydrophobic and amphipathic sequences, interact with phospholipid membranes where they exert a variety of activities in a lipid composition-dependent manner.[6,7] Such interactions result in the transmembrane passage of hydrophilic macromolecules, the formation of pores, transient openings or the stabilization of the membrane,[8,9] properties that are also of biomedical importance.[10,11]

Over the last 15 years, unnatural oligomers with folding patterns (*i.e.* foldamers [12]) akin to protein structure elements have gained considerable interest in the context of mimicking bioactive peptides and interacting with biomolecules (proteins, nucleic acids, phospholipid components of biological membranes, . . .).[13–16] Foldamers are endowed with properties (structural predictability, extended contact areas, diversity and resistance to proteolysis) that make them potentially useful as pharmacological tools to address some of the limitations of natural α-peptides. Reported applications of peptidomimetic foldamers range from inhibitors of protein–protein interaction to host-defense peptide mimics. Antimicrobial foldamers inspired by host-defense peptides include amphiphilic helical oligoamides such as β-peptides[17–19] and peptoids (oligomers of *N*-alkyl glycine),[20] extended arylamides [21] as well as non oligoamide foldamers such as aromatic and aliphatic N,N′-linked oligoureas.[22] Antibacterial oligoureas such as 8-mer **1** (Fig. 1) display significant antimicrobial activities against a broad spectrum of Gram-positive and Gram-negative bacteria.[23,24] They have been designed assuming an idealized 2.5-helical structure (*i.e.* 2.5 residues per turn), by sequestration of cationic residues on one face of the helix. The 2.5-helical structure of aliphatic urea foldamers has been thoroughly investigated for oligomers of various lengths in solution by diverse spectroscopic methods (NMR,[25–27] electronic circular dichroism (ECD),[28] FT-IR [29]) and in the crystal state by X-ray diffraction.[30,31] The helix is characterized by a (+)-synclinal arrangement around the main chain C–C bonds and is stabilized by a collection of three centered H-bonds closing 12- and 14-membered pseudo-rings.

Although steady-state fluorescence anisotropy measurements provided a first hint that antibacterial oligoureas such as **1** interact with phospholipid membranes,[24] the precise mechanism of their interaction with the membrane is still not well understood.

[a]*Université de Strasbourg/CNRS, UMR7177, Institut de Chimie, Faculté de chimie, 4 rue Blaise Pascal, 67070 Strasbourg, France. E-mail: bechinger@unistra.fr; Fax: +33 3 68 85 51 51; Tel: +33 3 68 85 51 50*
[b]*Université de Bordeaux-CNRS UMR5248, Institut Européen de Chimie et Biologie, 2 rue Robert Escarpit, 33607 Pessac, France. E-mail: g.guichard@iecb.u-bordeaux.fr*

† This article is part of an Organic & Biomolecular Chemistry web theme issue on Foldamer Chemistry.

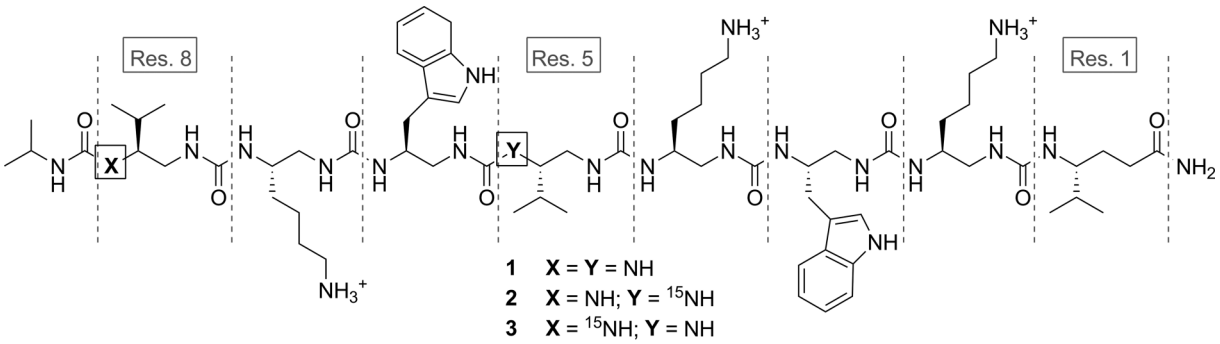

Fig. 1 Formula of reference antibacterial oligourea **1** and related oligomers **2** and **3** investigated in this study specifically ^{15}N-labelled at residue 5 and 8, respectively.

NMR spectroscopy is a proven method for the biophysical characterization of peptides, including their structure, dynamics and interactions in the presence of membranes.[32] This technique allows one to not only determine their conformation in many different environments, such as aqueous buffers, solvent mixtures or in the presence of micelles, but also to monitor their dynamics at high resolution and therefore their conformational plasticity.[3,32] The detailed description of the interaction properties of the NMR nuclei in the magnetic field of the NMR spectrometer in terms of interaction tensors has allowed for the development of elaborate solution state NMR techniques (*e.g.* residual dipolar couplings and residual chemical shift anisotropy) and for the detailed analysis of the dynamics and conformation of these polypeptides.[33–36] Furthermore, the knowledge of the size and molecular alignment of the tensor elements is a key requirement for the structural and dynamic analysis of solid-state NMR spectra. The nuclei located in the polypeptide backbone, such as the ^{15}N of the amide bond, have been proven to be particularly useful during the analysis of the structure and topology of labeled polypeptides when interacting with membranes.[32] Consequently, a large number of studies have been performed using this nucleus, with efforts to characterize the ^{15}N chemical shift tensor.[37] In particular, when investigated by static oriented solid-state NMR spectroscopy the ^{15}N chemical shift of membrane associated polypeptides has been shown to be directly correlated to the bilayer topology.[38]

By analogy to antibacterial α-peptides,[32] solid state NMR is likely to provide insight into the three-dimensional structure, dynamics and topology of amphiphilic oligoureas in lipid bilayers. Towards this end, in this paper we first determine the ^{15}N chemical shift tensor of the urea bond and thereafter present up-to-date solid-state NMR investigations revealing the membrane interactions of ^{15}N-labelled antimicrobial oligourea sequences (compounds **2** and **3**, Fig. 1) reconstituted into oriented phospholipid bilayers.

Results and discussion

NMR determination of the ^{15}N chemical shift tensor of a model diurea

In order to perform NMR spectroscopic investigations of oligourea foldamers, the tensor of the ^{15}N labelled backbone site was first determined using a simple ^{15}N-labelled diurea (**4**). The synthesis of **4** (Scheme 1) started from commercially available

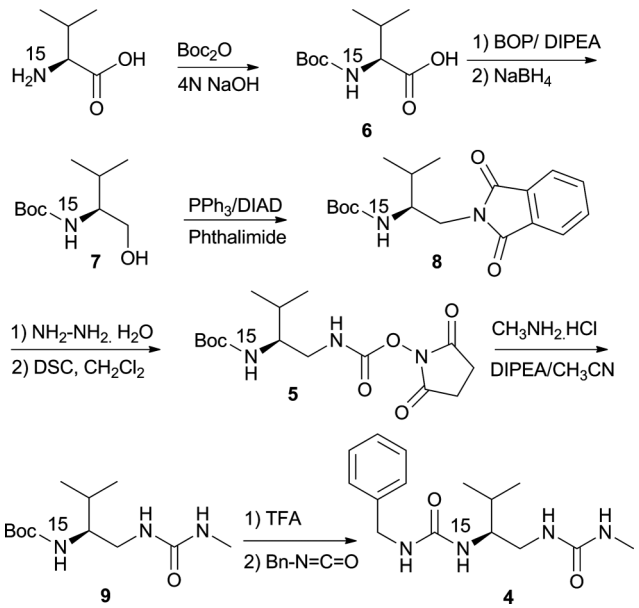

Scheme 1 Synthesis of ^{15}N-labelled succinimidyl carbamate **5** and model diurea **4**. BOP = benzotriazole-1-yl-oxy-tris-(dimethylamino)-phosphonium hexafluorophosphate; DIPEA = diisopropylethylamine; DIAD = diisopropyl azodicarboxylate; DSC = *N*,*N*′-disuccinimidyl carbonate; TFA = trifluoroacetic acid.

^{15}N-valine which was converted to [^{15}N]-(*R*)-succinimidyl-(2-(*tert*-butoxycarbonylamino)-3-methylbutyl)carbamate **5** with an overall yield of 49% (5 steps). The coupling of **5** with methylamine hydrochloride in the presence of diisopropylethylamine followed by Boc removal and reaction with benzyl isocyanate afforded **4** with a 81% yield.

The size of the main tensor elements of a labelled site within a polypeptide[39] or within an oligourea can be read from the discontinuities that are obvious in the one-dimensional chemical shift powder pattern (or the envelope describing the magic angle sample spinning (MAS) side band intensities) and the values obtained after the simulation of the spectrum obtained from **4** (Fig. 2B) are σ_{11} = 39 ppm, σ_{22} = 89 ppm and σ_{33} = 152 ppm (Fig. 2A). Determining their alignment within the molecular coordinate system is more demanding, and in the case of the ^{15}N amide bonds, this has been achieved by studies of single crystals, comparison to model compounds, quantum mechanical calculations[40,41] and more recently through two-dimensional

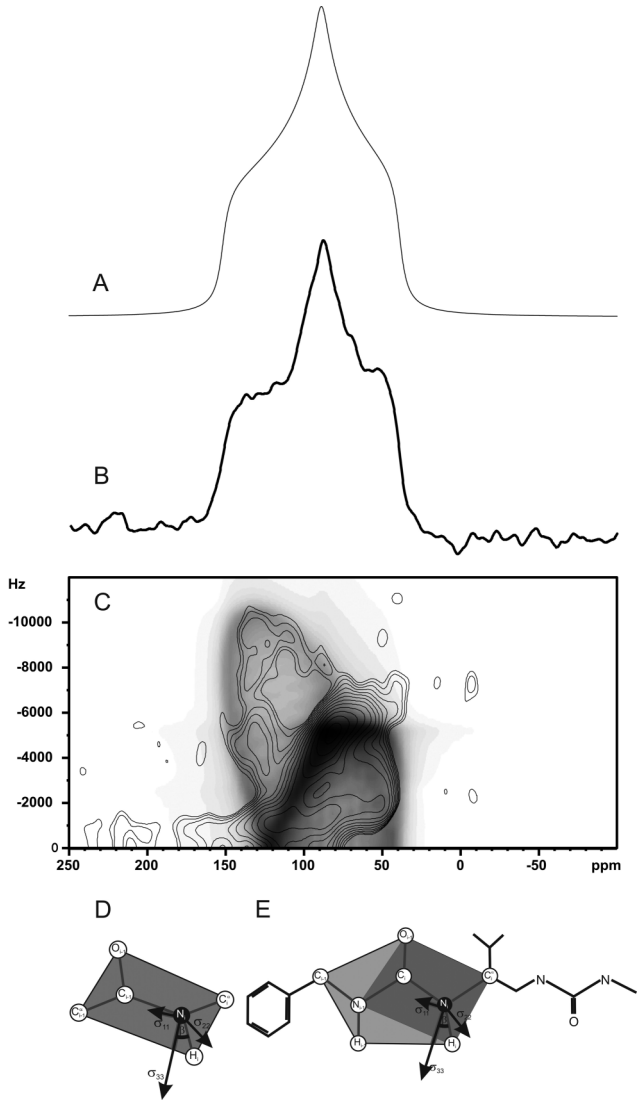

Fig. 2 A: Simulation of a 1D powder pattern using the principal values for the ^{15}N chemical shift tensor of σ_{11} = 39 ppm, σ_{22} = 89 ppm and σ_{33} = 152 ppm, and the orientation of the tensor as derived from the experiment shown in panel C and graphically presented in E. B: Proton-decoupled ^{15}N solid-state NMR spectrum of the model ^{15}N-labelled diurea **4**. C: The separated local field spectrum of **4** correlating the ^{15}N chemical shift and the ^{1}H-^{15}N dipolar coupling is shown by solid lines. The grey shading represents the simulated spectrum with α = 25°, σ_{11} = 39 ppm, σ_{22} = 89 ppm and σ_{33} = 152 ppm. Only the upper half of the symmetric spectrum is shown. D: representation of the ^{15}N chemical shift tensor of the peptide bond and E: of diurea **4**. In panels D and E the peptide bond and the corresponding structure in the urea bond are shown in dark grey. In panel E the areas in dark and light grey are shown as a continuous planar structure although the possibility of small deviations has been detected in more recent structural work.[30] For both molecules (D and E) the σ_{11} and σ_{33} main tensor elements are aligned within this plane.

solid-state NMR techniques on non-oriented samples (reviewed in references 37,42).

Fig. 2C shows the separated local field spectrum of the powder of the model compound **4**. The compound was designed in such a manner to represent all the chemical characteristics, and thereby the chemical shift properties, of an urea bond (Scheme 1). This two-dimensional spectrum correlates the ^{15}N chemical shift and the ^{1}H-^{15}N dipolar coupling of the individual molecules.[43] In this sample all molecular alignments are present in a random fashion (spherical distribution) and by adding up the spectral contributions, a two-dimensional powder pattern line shape is obtained; where the intensity distribution is a function of the relative alignment of the inter-atomic ^{1}H-^{15}N vector of the dipolar coupling and the ^{15}N chemical shift tensor.[43] The powder pattern line shape is characterized by two symmetry-related ellipsoid-like contributions, which add up into a "wing-like" distribution of resonance intensities (Fig. 2C).[44] The angle between the ^{1}H-^{15}N bond and σ_{33} is reflected in the eccentricity of the ellipsoidal resonance distribution, *i.e.* for σ_{33} parallel to the N–H vector the two-dimensional spectrum reduces to lines that cross each other at the isotropic chemical shift and dipolar coupling (93 ppm/0 kHz), whereas for σ_{33} perpendicular to ^{1}H-^{15}N a round spectral line shape is obtained. Computer simulations indicate that the observed spectral line shape (Fig. 2C) fits well to an angle of 25° covered by the ^{1}H-^{15}N bond and σ_{33}. The main tensor elements and this geometrical arrangement are illustrated in Fig. 2E. Although other symmetry-related arrangements cannot *a priori* be excluded from the spectral analysis alone, the close chemical relationship between the amide and urea bonds suggests that the urea bond tensor alignment is related to that of the peptide bond (Fig. 2D, E). In the latter case the angle covered by σ_{33} and the N–H vector amounts on average to 18° (recently reviewed in reference 37). The modest difference in the average tensor alignment between the two compounds ranges within the variance observed when the tensors of a large variety of peptide bonds have been analyzed.

However, when compared to the peptide bond (Fig. 2D) the higher shielding in the plane of the urea bond (Fig. 2E) and the concomitant reduction of the main tensor elements σ_{11} and σ_{33} is probably due to the extra electron density carried by the non-bonding electrons of the nitrogen which takes a position equivalent to the $C\alpha_{i-1}$ atom of the peptide bond.

Solid-state NMR analysis of ^{15}N-labelled antibacterial oligoureas

In the next step, octamer **2**, an analogue of antibacterial oligourea **1** specifically ^{15}N-labelled at residue 5 as indicated in Fig. 1, was reconstituted into phospholipid bilayers that are mechanically oriented along glass surfaces with their membrane normal parallel to the magnetic field direction.[45] The resulting separated local field spectrum representing the resonances of residue 5 is shown in Fig. 3B (black line) and compared to the powder pattern line shape of model compound **4** (Fig. 3B gray lines and Fig. 2C). The spectrum consists of a single peak pair at 59 ppm and a ^{1}H-^{15}N dipolar coupling of 5.2 kHz. Oligourea **3** labeled at position 8 leads to a similar spectrum with a peak at 83 ppm and a dipolar splitting of 4.4 kHz (not shown).

In order to determine the oligourea alignments relative to the membrane normal/B_o field that are in agreement with these two experimental parameters, the analysis of topological constraints, that has already proven highly successful with L-amino acid polypeptides,[32,46,47] was adapted by taking into consideration the structure and tensor of the oligourea bond (Fig. 2E). To evaluate which of the membrane alignments agree with the experimental measurements, the backbone of the previously solved crystal structure of a helical octaurea with benzyl side chains (CCDC 750017)[30] was used as a template onto which was modeled the

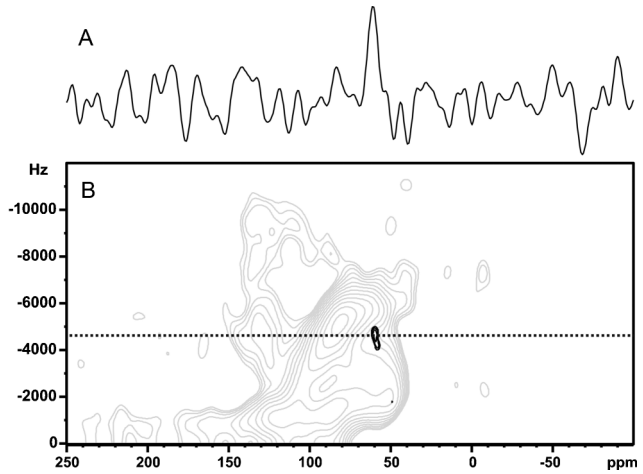

Fig. 3 ^{15}N separated local field spectrum of the labelled octaurea **2** reconstituted into uniaxially oriented 1-palmitoyl-2-oleoyl-*sn*-glycero-3-phosphocholine (POPC) bilayers. Whereas panel B shows the two-dimensional spectrum, panel A presents the trace at 4800 Hz (dotted line in B). The membrane normal is aligned parallel to the magnetic field direction of the NMR spectrometer. The experimental powder pattern line shape of compound **4** is shown in light grey for comparison (Fig. 2C).

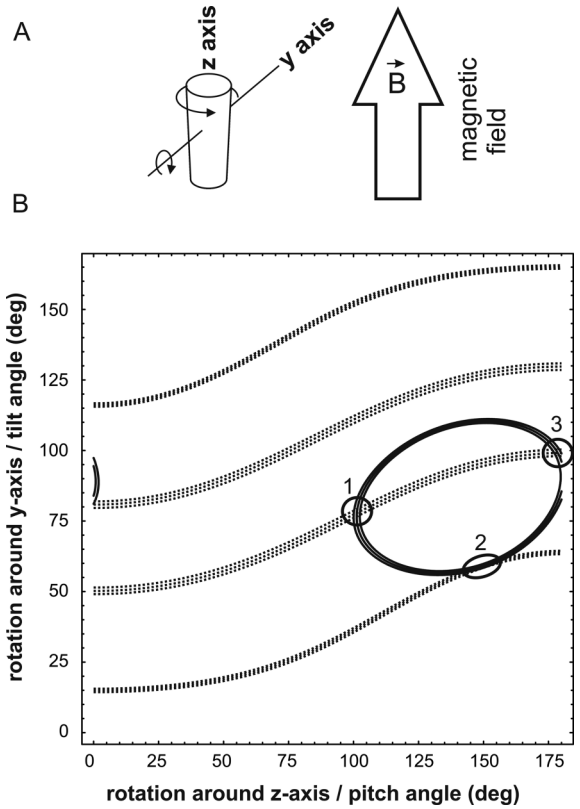

Fig. 4 Analysis of the possible membrane alignments of octaurea **2** that agree with the experimental solid-state NMR spectrum shown in Fig. 3. A: The initial positioning of the helix axis of **2** (*z*-axis) parallel to the magnetic field direction and the definition of the rotation axes. (B) Orientational constraints of **2** that arise from the experimental ^{15}N chemical shift (solid line) and the ^{15}N-^{1}H dipolar coupling (dashed line).

amphipathic distribution of side chains of the antibacterial oligourea **1**. As a starting configuration, the helix long axis was oriented parallel to the *z*-axis, which coincides with the membrane normal and B_o, thereby following previous protocols.[48,49] Thereafter the oligomer was rotated first around the *z*-axis (thereby changing the pitch angle) and then around the *y*-axis (thereby changing the helical tilt angle) (Fig. 4A). For each alignment thus obtained the corresponding chemical shift and dipolar coupling of the Val-type residue at position 5 was calculated and compared to the experimental spectrum. In Fig. 4B the orientations which agree with the experimental chemical shift of the ^{15}N labeled site within residue 5 (59 ±1 ppm) are represented by the black solid lines and alignments that agree with the dipolar splitting of 5.1 ±0.1 kHz are shown by the dashed traces. When the two restriction plots are combined with each other, only three intersections are obtained (marked 1, 2 and 3 in Fig. 4B) and these are the only oligourea alignments that are consistent with both ^{15}N chemical shift and the ^{15}N-^{1}H dipolar coupling of the residue 5 labeled site.

The configurations relative to the membrane surface corresponding to these alignments are shown in Fig. 5 as molecular models. Whereas alignment 1 (Fig. 5A) results in a perfect placement of the hydrophilic and hydrophobic residues in the corresponding environments, orientations 2 and 3 (Fig. 5B, C) place an amino alkyl (lysine type) side chain (shown in blue) in the membrane interior. Therefore the configuration 1 is likely to be the energetically more probable orientation. At the same time this in-planar configuration agrees with the physico-chemical properties of this amphipathic molecule and provides qualitative confirmation of the tensor characterization (Fig. 2).

When the NMR spectra of compound **3** (not shown) are taken into consideration, the topological analysis of this site agrees with an in-planar alignment but different tilt/pitch angular pairs are obtained when compared to the labeled residue 5. It should be noted however that the topological calculations use the pdb-coordinates from the crystal structure of a related octaurea compound (CCDC 750017)[30] and that the label at position 8 is very close to the terminus of the helical structure, a region of the oligourea where structural differences are likely to occur when the conformations in the crystal and the membrane are compared to each other. This is also supported by previous findings showing that the helix tends to fray at this end.[26,30]

In the case of α-peptides, it has been shown that due to unique tensor properties, including the alignment of the unique tensor element σ_{33} almost parallel to the long axis of α-helical domains, the ^{15}N chemical shift provides a direct indicator of the membrane alignment of these helices.[38] As a consequence, chemical shifts around 200 ppm (*i.e.* close to σ_{33}) are indicative of transmembrane helices and values <100 pm (*i.e.* in the range of σ_{11} and σ_{22}) are characteristic of helices alignments close to parallel to the surface.[38,50]

Therefore, we simulated the possible ^{15}N chemical shift/^{1}H-^{15}N dipolar coupling spectra that result from oligourea helix alignments of different tilt angles. We focused on alignments that are within 15° from perfect in-planar and transmembrane configurations (Fig. 6). Notably, as with labeled peptide bonds for each tilt angle a wheel-like distribution of chemical shift/dipolar couplings is obtained, the exact resonance position being dependent on the position of the ^{15}N label and the rotational pitch angle (*i.e.* rotation around *z* in Fig. 4A). As with α-peptides, transmembrane alignments exhibit chemical shift values close to σ_{33} whereas

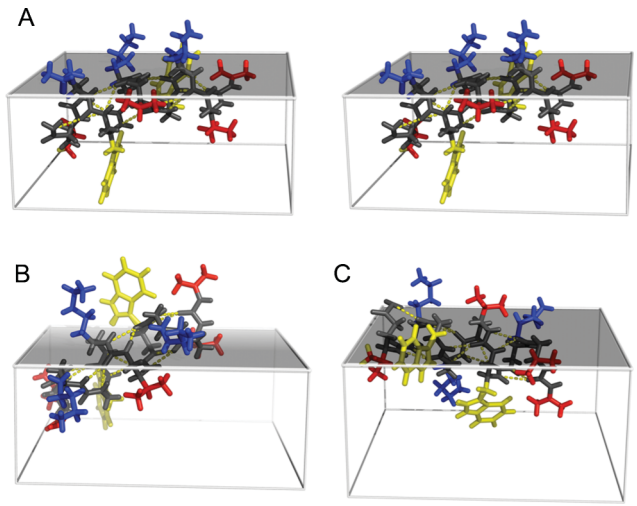

Fig. 5 Illustration of the molecular alignments that are consistent with ^{15}N chemical shift and ^{15}N-^{1}H dipolar coupling (*cf.* Fig. 3 and 4). Panel A corresponds to a stereo view of alignment 1 in Fig. 4, panels B and C to alignments 2 and 3, respectively. The amino alkyl (Lys type) side chains are displayed in blue, the isopropyl (Val type) side chains in red and indole (Trp type) in yellow. The hydrogen binding network is indicated by yellow lines. The lipid membranes are symbolized by a box with a semi-transparent surface.

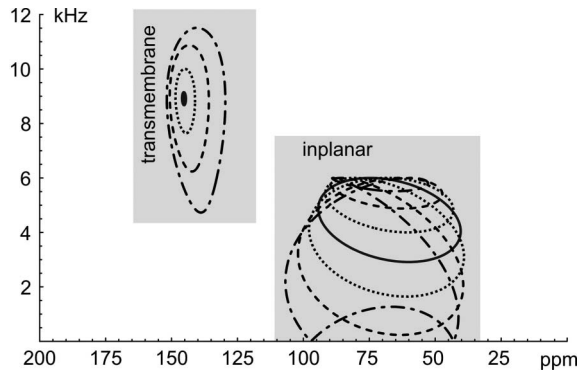

Fig. 6 Simulations of the polarization inversion spin exchange at the magic angle (PISEMA) spectra for an oligourea helix in in-planar and transmembrane configurations. The lines represent the possible peak positions, the exact resonance being a function of the position of the ^{15}N label relative to the rotational pitch angle. The black dot and line correspond to perfect transmembrane and in-plane alignments, respectively. The interrupted lines show the changes in the spectral properties when the tilt angle deviates from these perfect alignments in steps of 5°. Tilt angle of the transmembrane conformation: solid black: 0°, dotted grey: 5°, dashed grey: 10°, dashed-dotted grey: 15°. Tilt angle for the in-planar configuration: solid black: 90°, dotted grey: 85°, dashed grey: 80°, dashed-dotted grey: 75°.

in-plane orientations show ^{15}N chemical shifts in the range of σ_{11} and σ_{22}. Fig. 6 shows that indeed the ^{15}N chemical shift alone allows one to deduce the membrane alignment of oligoureas in a semi-quantitative manner. When the angular restraints from ^{15}N chemical shift and/or ^{1}H-^{15}N dipolar coupling are combined with each other the two parameters exhibit good complementarity and only a few well-defined angular pairs of tilt and rotational pitch angles are obtained (Fig. 4). This is in contrast to α-peptides where these two parameters combined in most cases do not provide information about the rotational pitch angle (Fig. 2D in [32]).

Finally, it should be noted that cationic amphipathic antimicrobial peptides have inspired the design of the promising helical peptidomimetics presented also in this work.[23,51] Both classes of compounds are characterized by amphipathic helical structures that align parallel to the membrane surface, which suggests that they also share a closely related mechanism for their antimicrobial action.[51,52]

Conclusions

Here, for the first time, antimicrobial oligoureas[23,24] carrying ^{15}N labeled backbone sites have been prepared and the ^{15}N chemical shift tensor of a related model compound has been determined. Knowledge of the main tensor elements and their alignment within the molecular coordinate system is a prerequisite to perform NMR experiments in which the structure, dynamics, interactions and topology of the oligourea foldamer can be investigated.

Using this information the association of an antimicrobial amphipathic oligourea with oriented lipid membranes was studied successfully and a surface alignment was obtained analogous to observations made of amphipathic helical polypeptides such as model sequences,[53,54] magainins[7,50,55] or other antimicrobial peptides.[56–59] Both topologies that agree with the experimental constraints (Fig. 4 and 5) correspond to (approximately) in-planar orientations, and are in agreement with previous studies on amphipathic polypeptide helices.

Experimental

1. General

Thin layer chromatography (TLC) was performed on silica gel 60 F254 (Macherey-Nagel) with detection by UV light and charring with 1% w/w ninhydrin in ethanol followed by heating. Flash column chromatography was carried out on silica gel (0.063–0.200 nm). Reverse phase (RP) HPLC analysis was performed on a Nucleosil C18 column (4.6 × 150 mm, 100 Å, 5 μm) (Macherey Nagel) using a linear gradient of A (0.1% TFA in H_2O) and B (0.08% TFA in CH_3CN) at a flow rate of 1.2 mL min^{-1} with UV detection at 214 nm. Unless specified, the HPLC gradient used is 30–100% B in 20 min. ^{1}H NMR and ^{13}C NMR spectra were recorded using a Bruker Advance DPX-300. Mass spectra were recorded using an LCQ Advantage Max (Thermo Fisher Scientific) mass spectrometer coupled to a surveyor plus HPLC (Thermo Fisher Scientific) system using a Nucleodur C_{18} (2 × 100 mm, 100 Å, 3 μm) column (Macherey Nagel) with a linear gradient of A (0.1% formic acid in H_2O) and B (CH_3CN LC/MS grade). When not specified, the gradient used is 30–100% B in 10 min. Boc-γ^4-Val-OH was prepared as described.[60] Activated monomers with side chains of Val, Trp and Lys were prepared using a previously described procedure.[24,61]

2. Experimental procedure for the synthesis of ^{15}N labelled activated building block with isopropyl (Val type) side chain

***N*-Boc protected [^{15}N]-L-Valine (6).** To (*S*)-^{15}N-2-amino-3-methyl butanoic acid (1.0 g, 8. 46 mmol) at 0 °C, a 4 N NaOH (2.13 mL) solution was added followed by $(Boc)_2O$ (2.03 mL,

9.31 mmol). The reaction was stirred overnight. The reaction mixture was acidified with 1 N $KHSO_4$ solution, diluted with EtOAc and the organic phase was dried over the $NaSO_4$ and evaporated to give Boc-[^{15}N]-Val-OH **6** (1.8 g, 98%) as white solid.

[^{15}N]-2-*tert*-Butoxycarbonyl-L-valinol (7). To a cold solution of **6** (1.8 g, 8.25 mmol) in THF (20 mL) were successively added benzotriazole-1-yl-oxy-tris-(dimethylamino)-phosphonium hexafluorophosphate (BOP) (4.01 mL, 9.08 mmol) and diisopropylethylamine (DIPEA) (1.68 mL, 9.9 mmol). After 15 min, sodium borohydride (0.312 g, 8.25 mmol) was added and the reaction mixture was stirred for 20 min. THF was evaporated from the reaction mixture and diluted with EtOAc. The organic layer was washed with 2 × 20 mL saturated $NaHCO_3$ solution, dried over $NaSO_4$, and evaporated. The residue was purified by column chromatography (silica gel, 30% EtOAc in cyclohexane) to give **7** (1.42 g, 84%) as a white solid; ^{1}H NMR (300 MHz, $CDCl_3$) δ = 4.83 (d, J = 7.9 Hz, ^{15}NH), 4.53 (d, J = 7.9 Hz, ^{15}NH), 3.73–3.54 (m, 2H), 3.49–3.32 (m, 1H), 2.23 (br s, OH), 1.90–1.73 (m, 1H), 1.44 (s, 9H), 0.94 (d, J = 6.5 Hz, 3H), 0.92 (d, J = 6.5 Hz, 3H).

[^{15}N]-(*R*)-*tert*-butyl(1-(1,3-dioxoisoindolin-2-yl)-3-methylbutan-2-yl)carbamate (8). To a solution of **7** (1.42 g, 6.96 mmol) in dry THF (15 mL) at 0 °C, were added phthalimide (1.12 g, 7.65 mmol), and triphenylphosphine (1.92 g, 7.3 mmol), followed by diisopropyl azodicarboxylate (DIAD) (1.47 mL, 7.3 mmol). After 2 h, THF was evaporated from the reaction mixture and diluted with CH_2Cl_2 and cyclohexane. The yellow precipitate which formed was filtered and the residue was washed with Et_2O and purified by column chromatography (silica gel, 15% EtOAc in cyclohexane) to give **8** (2.1 g, 92%) as a white solid; ^{1}H NMR (300 MHz, $CDCl_3$) δ = 7.87–7.78 (m, 2H), 7.71–7.65 (m, 2H), 4.67 (d, J = 9.7 Hz, ^{15}NH), 4.37 (d, J = 9.7 Hz, ^{15}NH), 3.92–3.80 (m, 1H), 3.75–3.64 (m, 2H), 1.91–1.74 (m, 1H), 1.15 (s, 9H), 1.0 (d, J = 7.0 Hz, 3H), 0.98 (d, J = 7.0 Hz, 3H).

[^{15}N]-(*R*)-*O*-succinimidyl-(2-(*tert*-butoxycarbonylamino)-3-methylbutyl)carbamate (5). To a warm (~70° C) solution of **8** (2.1 g, 6.3 mmol) in MeOH (20 mL), was added hydrazine hydrate (0.93 mL, 18.9 mmol) and the reaction mixture was stirred overnight. The reaction mixture was filtered through a sintered funnel, the MeOH evaporated and the residue was diluted with CH_2Cl_2. The organic layer was washed with a saturated $NaHCO_3$ solution and dried over Na_2SO_4. The solvent was evaporated under reduced pressure to give the free amine (1.04 g) as a yellow syrup which was used as such for the next step without purification. A solution of the amine in CH_2Cl_2 (10 mL) was added to a solution of *N*,*N*′-disuccinimidyl carbonate (1.57 g, 6.14 mmol) in CH_2Cl_2 (20 mL) and the reaction mixture was stirred for 15 min. The precipitate which formed was filtered and the residue was washed with CH_2Cl_2 and 3 × 20 mL of 1 N $KHSO_4$. The organic layer was dried over $NaSO_4$ and evaporated to give **5** (1.4 g, 65%) as a white solid; ^{1}H NMR (300 MHz, $CDCl_3$) δ = 6.17–6.07 (m, 1NH), 4.58 (d, J = 9.1 Hz, ^{15}NH), 3.61–3.49 (m, 1H), 3.44–3.19 (m, 2H), 2.80 (s, 4H), 1.84–1.71 (m, 1H), 1.44 (s, 9H), 0.96 (d, J = 7.0 Hz, 3H), 0.93 (d, J = 7.0 Hz, 3H).

3. Experimental procedure for the synthesis of ^{15}N labelled model diurea (4)

[^{15}N]-(*R*)-*tert*-butyl (3-methyl-1-(3-methylureido)butan-2-yl)carbamate (9). To a stirred solution of $HCl{\cdot}NH_2CH_3$ (0.058 g, 0.872 mmol) in CH_3CN (4 mL) at 0° C, was added DIPEA (0.3 mL, 1.74 mmol), followed by **5** (0.2 g, 0.581 mmol) after 5 min. The reaction mixture was diluted with EtOAc and the organic layer was washed with a saturated $NaHCO_3$ solution, 1 N $KHSO_4$, water and brine. The organic layer was dried over $NaSO_4$ and evaporated to yield **9** (0.135 g, 89%) as a white solid; ^{1}H NMR (300 MHz, $CDCl_3$) δ = 5.14–5.01 (m, 1NH), 4.85 (d, J = 9.1 Hz, ^{15}NH), 4.76–4.67 (m, 1NH), 4.55 (d, J = 9.1 Hz, ^{15}NH), 3.51–3.39 (m, 1H), 3.35–3.12 (m, 2H), 2.76–2.73 (m, 3H), 1.81–1.69 (m, 1H), 1.42 (s, 9H), 0.94 (d, J = 7.0 Hz, 3H), 0.92 (d, J = 7.0 Hz, 3H).

[^{15}N]-(*R*)-1-benzyl-3-(3-methyl-1-(3-methylureido)butan-2-yl) urea (4). Compound **9** (0.095 g, 0.37 mmol) was treated with trifluoroacetic acid (TFA) (1 mL) at 0° C for 30 min. Concentration under reduced pressure and co-evaporation with cyclohexane left a residue which was dried under high vacuum. To a stirred solution of the resulting TFA salt in CH_3CN (2 mL) was added DIPEA (0.13 mL, 0.73 mmol), and after 10 min the reaction mixture was treated with benzyl isocyanate (0.051 g, 0.38 mmol) and stirred for 1 h. The reaction was concentrated and upon addition of a saturated $NaHCO_3$ solution, a precipitate formed. It was collected and washed with saturated $NaHCO_3$ solution, water, 1 N $KHSO_4$, water and further washed with cyclohexane and n-pentane to remove the non-polar impurities and finally dried under high vacuum to give **4** (0.097 g, 91%) as a white solid; ^{1}H NMR (300 MHz, CD_3OH) δ = 7.34–7.18 (m, 5H), 6.44–6.34 (m, NH), 5.94–5,84 (m, 2NH), 5.62 (d, J = 9.4 Hz, 1NH), 4.34–4.26 (m, 2H), 3.64–3.51 (m, 1H), 3.24–3.06 (m, 2H), 2.65 (d, J = 4.6 Hz, 3H), 1.83–1.65 (m, 1H), 0.93 (d, J = 7.0 Hz, 3H), 0.90 (d, J = 7.0 Hz, 3H).

4. Synthesis of ^{15}N labelled urea oligomer 2 and 3

General Procedure. ^{15}N labelled urea oligomer **2** and **3** were synthesized using Boc chemistry on a multichannel synthesizer with a semi-automatic mode on a 100 μmol scale starting from 4-methylbenzhydrylamine (MBHA) resin (0.62 mmol g^{-1}). The first coupling step was performed with a solution of Boc-protected γ^4-Val-OH (1.5 eq.) in DMF, with BOP (1.5 eq.), HOBt (1.5 eq.) and DIPEA (5 eq.) and the suspension was mixed under periodic nitrogen bubbling for 30 min. The coupling was performed twice and completion was monitored by a Kaiser ninhydrin test. For each following coupling step, a solution of the succinimidyl carbamate building block with a side chain of either Val, Trp or Lys(2-Cl-Z) (3 eq.) or ^{15}N labelled succinimidyl carbamate derivative **5** (3 eq.) and DIPEA (6 eq.) in DMF was added on the resin, and the suspension was mixed under periodic nitrogen bubbling for 120 min. A double coupling was performed systematically. The Boc group was removed using TFA (5 and 10 min) under nitrogen bubbling. The resin was then filtered and washed with DMF (5 × 1 min). Acylation of the terminal amino group of the oligourea was performed in DMF, in the presence of isopropyl isocyanate (3 eq.) and DIPEA (5 eq.) and the suspension was mixed under periodic nitrogen bubbling for 30 min. At the end of the synthesis, the resin was washed with CH_2Cl_2, Et_2O

and dried under nitrogen. Side chain deprotection and cleavage of the oligomer from the resin were performed simultaneously by treatment with HF (containing 10% *p*-cresol as a scavenger) for 60 min at 0 °C. The crude oligomers were finally purified by RP-HPLC (linear gradient, 20–80% B, 30 min) to a final purity ≥95% and lyophilized.

[^{15}N] labelled oligourea 2. Synthesis on 100 μmol scale. Purity of crude product >55% (C_{18} RP-HPLC). Yield after purification: (35 mg, 31%); White powder; RP-HPLC t_R 14.48 min (linear gradient, 20–80% B, 30 min); MS (ES+) m/z 1388.3 $[M + H]^+$.

[^{15}N] labelled oligourea 3. Synthesis on 100 μmol scale. Purity of crude product >70% (C_{18} RP-HPLC). Yield after purification: (35 mg, 33%); White powder; RP-HPLC t_R 14.21 min (linear gradient, 20–80% B, 30 min); MS (ES+) m/z 1388.3 $[M + H]^+$.

5. Preparation of oriented membranes for solid-state NMR measurement

Uniaxially oriented samples for solid-state NMR spectroscopy were prepared, as described in detail previously,[45] by co-dissolving 10 mg of ^{15}N labelled oligourea **2** or **3** and 200 mg of 1-palmitoyl-2-oleoyl-*sn*-glycero-3-phosphocholine (POPC) in ~1 mL trifluoroethanol. Most of the organic solvent was slowly evaporated with a stream of nitrogen and the remainder volume of about 200 μL was spread onto ultra-thin cover glasses (8 × 11 mm from Marienfeld, Lauda-Königshofen, Germany). After drying on air, the samples were exposed to high vacuum overnight to remove all traces of the organic solvents. The membranes were equilibrated at 93% relative humidity, before stacking the glass-plates on top of each other. Finally, the stacks were stabilized with Teflon tape, sealed with a polyethylene plastic wrapping[45] and inserted into a commercial flat coil[62] e-free double-resonance probe head (Bruker Biospin Rheinstetten, Germany) in such a manner that the glass plate normal is oriented parallel to the magnetic field direction of the NMR spectrometer (B_o).

6. Solid state NMR measurements

The one-dimensional proton-decoupled ^{15}N solid-state NMR spectra were obtained on an Avance wide-bore spectrometer operating at 11.8 Tesla (Bruker Biospin Rheinstetten, Germany) using cross-polarization with B_1 fields of 41 kHz. The ^{1}H-^{15}N cross-polarization was applied for 3 ms using adiabatic passage through the Hartmann–Hahn condition [63] and the spinal64 sequence for proton decoupling.[64]

Two dimensional chemical shift/heteronuclear dipolar coupling spectra were recorded on an Avance wide-bore spectrometer operating at 9.4 Tesla (Bruker Biospin Rheinstetten, Germany) using the polarization inversion spin exchange at the magic angle (PISEMA) pulse sequence.[44] Briefly, after a cross polarization contact time of 800 μs in which magnetisation is transferred from ^{1}H to ^{15}N, the ^{1}H-^{15}N dipolar coupling is encoded during the application of a SEMA series of frequency- and phase-switched 2π pulses. The ^{1}H- and ^{15}N- B_1 fields during cross polarization were 83 kHz. Within the SEMA pulse train the effective ^{1}H/^{15}N fields were 70 kHz using a ^{1}H frequency offset of ±40.415 kHz. The scaling factor of the PISEMA experiment (0.82) was taken into account during spectral processing.[44]

7. Analysis and simulation of NMR spectra using Mathematica and SIMPSON

Contour plots of the type in Fig. 4 were created using Mathematica 3.1 (Wolfram Research, Champaign, Il, USA). The tensor for the labeled nitrogen was placed inside the coordinate system of the pdb file. Rotations of the tensors first around the *z*-axis and then around the *y*-axis were performed with the angles as variables in an analytical form. The chemical shift or dipolar coupling were calculated for a B-field in the *z*-direction as a function of the rotation angles. Then the contour plot function of Mathematica was used to show the orientations, where the chemical shift values agree with the measured value.

The simulations of the 1D- and the PISEMA powder patterns were performed using SIMPSON.[65] In the case of the 1D simulation a simple 90°- acquisition program was used, whereas for the simulation of the 2D-PISEMA spectra the full pulse-program was used. Powder averaging was active by using "powder-crystal files" (zcw986 for the PISEMA and zcw28656 for the 1D).

Acknowledgements

We are grateful for the financial support from the Agence National de la Recherche (TRANSPEP project ANR-07-PCVI-0018), Vaincre la Mucoviscidose, the University of Strasbourg (PPF RMN), the University of Bordeaux, the Région Aquitaine, the French Ministry of Research and the CNRS.

References

1 A. Naito and K. Nishimura, *Curr. Top. Med. Chem.*, 2004, **4**, 135–145.
2 K. A. Brogden, J. M. Guthmiller, M. Salzet and M. Zasloff, *Nat. Immunol.*, 2005, **6**, 558–564.
3 E. F. Haney, H. N. Hunter, K. Matsuzaki and H. J. Vogel, *Biochim. Biophys. Acta, Biomembr.*, 2009, **1788**, 1639–1655.
4 B. Bechinger, V. Vidovic, P. Bertani and A. Kichler, *J. Pept. Sci.*, 2011, **17**, 88–93.
5 L. Maler and A. Graslund, *Methods Mol. Biol.*, 2011, **683**, 57–67.
6 R. Sauder, J. Seelig and A. Ziegler, *Methods Mol. Biol.*, 2011, **683**, 129–155.
7 E. Salnikov and B. Bechinger, *Biophys. J.*, 2011, **100**, 1473–1480.
8 B. Bechinger and K. Lohner, *Biochim. Biophys. Acta, Biomembr.*, 2006, **1758**, 1529–1539.
9 S. Deshayes, K. Konate, G. Aldrian, L. Crombez, F. Heitz and G. Divita, *Biochim. Biophys. Acta, Biomembr.*, 2010, **1798**, 2304–2314.
10 E. B. Hadley and R. E. Hancock, *Curr Top Med Chem*, 2010, **10**, 1872–1881.
11 R. M. Johnson, S. D. Harrison and D. Maclean, *Methods Mol. Biol.*, 2011, **683**, 535–551.
12 S. H. Gellman, *Acc. Chem. Res.*, 1998, **31**, 173–180.
13 D. Seebach, A. K. Beck and D. J. Bierbaum, *Chem. Biodiversity*, 2004, **1**, 1111–1239.
14 C. M. Goodman, S. Choi, S. Shandler and W. F. DeGrado, *Nat. Chem. Biol.*, 2007, **3**, 252–262.
15 S. Hecht and I. E. Huc, *Foldamers: Structure, Properties and Applications*, Wiley-VCH, Weinheim, 2007.
16 G. Guichard and I. Huc, *Chem. Commun.*, 2011, **47**, 5933–5941.
17 Y. Hamuro, J. P. Schneider and W. F. DeGrado, *J. Am. Chem. Soc.*, 1999, **121**, 12200–12201.
18 E. A. Porter, X. Wang, H. S. Lee, B. Weisblum and S. H. Gellman, *Nature*, 2000, **404**, 565.
19 P. I. Arvidsson, N. S. Ryder, H. M. Weiss, G. Gross, O. Kretz, R. Woessner and D. Seebach, *ChemBioChem*, 2003, **4**, 1345–1347.
20 N. P. Chongsiriwatana, J. A. Patch, A. M. Czyzewski, M. T. Dohm, A. Ivankin, D. Gidalevitz, R. N. Zuckermann and A. E. Barron, *Proc. Natl. Acad. Sci. U. S. A.*, 2008, **105**, 2794–2799.
21 G. N. Tew, R. W. Scott, M. L. Klein and W. F. Degrado, *Acc. Chem. Res.*, 2010, **43**, 30–39.

22 L. Fischer and G. Guichard, *Org. Biomol. Chem.*, 2010, **8**, 3101–3117.
23 A. Violette, S. Fournel, K. Lamour, O. Chaloin, B. Frisch, J. P. Briand, H. Monteil and G. Guichard, *Chem. Biol.*, 2006, **13**, 531–538.
24 P. Claudon, A. Violette, K. Lamour, M. Decossas, S. Fournel, B. Heurtault, J. Godet, Y. Mely, B. Jamart-Gregoire, M. C. Averlant-Petit, J. P. Briand, G. Duportail, H. Monteil and G. Guichard, *Angew Chem Int Ed Engl*, 2010, **49**, 333–336.
25 C. Hemmerlin, M. Marraud, D. Rognan, R. Graff, V. Semetey, J. P. Briand and G. Guichard, *Helv. Chim. Acta*, 2002, **85**, 3692–3711.
26 A. Violette, M. C. verlant-Petit, V. Semetey, C. Hemmerlin, R. Casimir, R. Graff, M. Marraud, J. P. Briand, D. Rognan and G. Guichard, *J. Am. Chem. Soc.*, 2005, **127**, 2156–2164.
27 G. Guichard, A. Violette, G. Chassaing and E. Miclet, *Magn. Reson. Chem.*, 2008, **46**, 918–924.
28 M. T. Oakley, G. Guichard and J. D. Hirst, *J. Phys. Chem. B*, 2007, **111**, 3274–3279.
29 D. Cavagnat, P. Claudon, L. Fischer, G. Guichard and B. Desbat, *J. Phys. Chem. B*, 2011, **115**, 4446–4452.
30 L. Fischer, P. Claudon, N. Pendem, E. Miclet, C. Didierjean, E. Ennifar and G. Guichard, *Angew. Chem., Int. Ed.*, 2010, **49**, 1067–1070.
31 J. Fremaux, L. Fischer, T. Arbogast, B. Kauffmann and G. Guichard, *Angew. Chem. Int Ed.*, 2011, **50**, 11382–11385.
32 B. Bechinger, J. M. Resende and C. Aisenbrey, *Biophys. Chem.*, 2011, **153**, 115–125.
33 R. S. Lipsitz and N. Tjandra, *Annu. Rev. Biophys. Biomol. Struct.*, 2004, **33**, 387–413.
34 A. Bax and A. Grishaev, *Curr. Opin. Struct. Biol.*, 2005, **15**, 563–570.
35 J. H. Prestegard, C. M. Bougault and A. I. Kishore, *Chem. Rev.*, 2004, **104**, 3519–3540.
36 J. R. Tolman and K. Ruan, *Chem. Rev.*, 2006, **106**, 1720–1736.
37 E. Salnikov, P. Bertani, J. Raap and B. Bechinger, *J. Biomol. NMR*, 2009, **45**, 373–387.
38 B. Bechinger and C. Sizun, *Concepts Magn. Reson.*, 2003, **18A**, 130–145.
39 E. S. Salnikov, H. Friedrich, X. Li, P. Bertani, S. Reissmann, C. Hertweck, J. D. O'Neil, J. Raap and B. Bechinger, *Biophys. J.*, 2009, **96**, 86–100.
40 J. R. Brender, D. M. Taylor and A. Ramamoorthy, *J. Am. Chem. Soc.*, 2001, **123**, 914–922.
41 A. Poon, J. Birn and A. Ramamoorthy, *J. Phys. Chem. B*, 2004, **108**, 16577–16585.
42 H. Saito, I. Ando and A. Ramamoorthy, *Prog. Nucl. Magn. Reson. Spectrosc.*, 2010, **57**, 181–228.
43 C. H. Wu, A. Ramamoorthy, L. M. Gierasch and S. J. Opella, *J. Am. Chem. Soc.*, 1995, **117**, 6148–6149.
44 A. Ramamoorthy, Y. Wei and D. Lee, *Annu. Rep. NMR Spectrosc.*, 2004, **52**, 1–52.
45 B. Bechinger, P. Bertani, S. Werten, C. Mendonca de Moraes, C. Aisenbrey, A. J. Mason, B. Perrone, M. Prudhon , U. S. Sudheendra, V. Vidovic and C. Miguel, in: *Membrane-active peptides: Methods and results on structure and function*, International University Line, La Jolla, California, USA, 2010, pp. 196–215.
46 C. Aisenbrey, C. Sizun, J. Koch, M. Herget, U. Abele, B. Bechinger and R. Tampe, *J. Biol. Chem.*, 2006, **281**, 30365–30372.
47 J. M. Resende, C. Mendonca Moraes, V. H. D. O. Munhoz, C. Aisenbrey, R. M. Verly, P. Bertani, A. Cesar, D. Pilo-Veloso and B. Bechinger, *Proc. Natl. Acad. Sci. U. S. A.*, 2009, **106**, 16639–16644.
48 V. Wray, R. Kinder, T. Federau, P. Henklein, B. Bechinger and U. Schubert, *Biochemistry*, 1999, **38**, 5272–5282.
49 C. Aisenbrey and B. Bechinger, *Biochemistry*, 2004, **43**, 10502–10512.
50 B. Bechinger, *J. Pept. Sci.*, 2011, **17**, 306–314.
51 B. Bechinger, *Curr. Opin. Colloid Interface Sci.*, 2009, **14**, 349–355.
52 A. Ramamoorthy, *Solid State Nucl. Magn. Reson.*, 2009, **35**, 201–207.
53 T. C. B. Vogt, P. Ducarme, S. Schinzel, R. Brasseur and B. Bechinger, *Biophys. J.*, 2000, **79**, 2644–2656.
54 C. Aisenbrey, R. Kinder, E. Goormaghtigh, J. M. Ruysschaert and B. Bechinger, *J. Biol. Chem.*, 2006, **281**, 7708–7716.
55 K. J. Hallock, D. K. Lee and A. Ramamoorthy, *Biophys. J.*, 2003, **84**, 3052–3060.
56 R. Fu, M. Truong, R. J. Saager, M. Cotten and T. A. Cross, *J. Magn. Reson.*, 2007, **188**, 41–48.
57 A. J. Mason, P. Bertani, G. Moulay, A. Marquette, B. Perrone, A. F. Drake, A. Kichler and B. Bechinger, *Biochemistry*, 2007, **46**, 15175–15187.
58 A. J. Mason, W. Moussaoui, T. Abdelrhaman, A. Boukhari, P. Bertani, A. Marquette, P. Shooshtarizaheh, G. Moulay, N. Boehm, B. Guerold, R. J. H. Sawers, A. Kichler, M. H. Metz-Boutigue, E. Candolfi, G. Prevost and B. Bechinger, *J. Biol. Chem.*, 2009, **284**, 119–133.
59 U. H. Durr, U. S. Sudheendra and A. Ramamoorthy, *Biochim. Biophys. Acta, Biomembr.*, 2006, **1758**, 1408–1425.
60 M. Smrcina, P. Majer, E. Majerova, T. A. Guerassina and M. A. Eissenstat, *Tetrahedron*, 1997, **53**, 12867–12874.
61 G. Guichard, V. Semetey, C. Didierjean, A. Aubry, J. P. Briand and M. Rodriguez, *J. Org. Chem.*, 1999, **64**, 8702–8705.
62 B. Bechinger and S. J. Opella, *J. Magn. Reson.*, 1991, **95**, 585–588.
63 S. Hediger, B. H. Meier, N. D. Kurur, G. Bodenhausen and R. R. Ernst, *Chem. Phys. Lett.*, 1994, **223**, 283–288.
64 B. M. Fung, A. K. Khitrin and K. Ermolaev, *J. Magn. Reson.*, 2000, **142**, 97–101.
65 M. Bak, J. T. Rasmussen and N. C. Nielsen, *J. Magn. Reson.*, 2000, **147**, 296–330.